Published online 22 February 2020 *Nucleic Acids Research, 2020, Vol. 48, No. 7* **3553–3566**
doi: 10.1093/nar/gkaa108

Recombination may occur in the absence of transcription in the immunoglobulin heavy chain recombination centre

Chloé Oudinet, Fatima-Zohra Braikia, Audrey Dauba and Ahmed Amine Khamlichi*

Institut de Pharmacologie et de Biologie Structurale, IPBS, Université de Toulouse, CNRS, Université Paul Sabatier, 31077 Toulouse, France

Received December 08, 2019; Revised February 06, 2020; Editorial Decision February 07, 2020; Accepted February 19, 2020

ABSTRACT

Developing B cells undergo V(D)J recombination to generate a vast repertoire of Ig molecules. V(D)J recombination is initiated by the RAG1/RAG2 complex in recombination centres (RCs), where gene segments become accessible to the complex. Whether transcription is the causal factor of accessibility or whether it is a side product of other processes that generate accessibility remains a controversial issue. At the *IgH* locus, V(D)J recombination is controlled by Eμ enhancer, which directs the transcriptional, epigenetic and recombinational events in the *IgH* RC. Deletion of Eμ enhancer affects both transcription and recombination, making it difficult to conclude if Eμ controls the two processes through the same or different mechanisms. By using a mouse line carrying a CpG-rich sequence upstream of Eμ enhancer and analyzing transcription and recombination at the single-cell level, we found that recombination could occur in the RC in the absence of detectable transcription, suggesting that Eμ controls transcription and recombination through distinct mechanisms. Moreover, while the normally Eμ-dependent transcription and demethylating activities were impaired, recruitment of chromatin remodeling complexes was unaffected. RAG1 was efficiently recruited, thus compensating for the defective transcription-associated recruitment of RAG2, and providing a mechanistic basis for RAG1/RAG2 assembly to initiate V(D)J recombination.

INTRODUCTION

Developing B and T cells undergo a complex and ordered series of DNA rearrangements called V(D)J recombination that ultimately lead to the vast repertoire of antigen receptors. The process enables assembly of variable (V), diversity (D) and joining (J) gene segments into an exon that encodes the antigen-binding domain of antigen receptors. V(D)J recombination is initiated by the lymphoid-specific recombinase complex RAG, which recognizes recombination signal sequences (RSSs), consisting of relatively well-conserved heptamer and nonamer sequences separated by a less-conserved spacer of 12 or 23 bp (1,2).

V(D)J recombination is triggered when the RAG complex binds to the RSSs that flank V, D and J segments. The complex initiates double-strand breaks between the heptamer and the gene segment, followed by end processing and ligation by the classical nonhomologous end-joining pathway (3–5). The RAG complex is composed of the catalytic subunit RAG1 and the accessory factor RAG2. RAG1 interacts with both the heptamer and the nonamer and initiates DNA cleavage (2). Although RAG2 does not bind DNA directly, it is essential to DNA cleavage *via* its interaction with RAG1 and recognition of H3K4me3 mark through its plant homeodomain (PHD) (6–8). RAG1 and RAG2 are preferentially recruited to a small, enhancer-proximal region spanning the J region and (in the case of *IgH* and *Tcrb* loci) the closest D segment (9). This region, named recombination centre (RC) (9), is highly enriched in transcriptional activity and associated RNAp II occupancy and active chromatin modifications, which render RSSs readily accessible to the RAG complex (10,11).

Despite sequence conservation of the RSSs and the use of the same recombinase, *Ig* genes are fully assembled in developing B cells only and *Tcrs* are assembled in developing T cells only. This requires that the RSSs become accessible to the recombinase in the right cell type and at the right developmental stage (12–15). The concept of accessibility was initially proposed based on the finding that at the *IgH* locus tissue-specific, developmentally controlled transcription of unrearranged V_H gene segments, termed germline transcription, coincides with their targeting for recombination (16). This strongly suggested that transcription of unrearranged gene segments was part of the regulatory mechanisms that control RSS accessibility (16). Subsequent studies on the role of germline transcription in generating RSS

*To whom correspondence should be addressed. Tel: +33 5 61 17 55 22; Fax: +33 5 61 17 59 97; Email: ahmed.khamlichi@ipbs.fr

© The Author(s) 2020. Published by Oxford University Press on behalf of Nucleic Acids Research.
This is an Open Access article distributed under the terms of the Creative Commons Attribution Non-Commercial License (http://creativecommons.org/licenses/by-nc/4.0/), which permits non-commercial re-use, distribution, and reproduction in any medium, provided the original work is properly cited. For commercial re-use, please contact journals.permissions@oup.com

accessibility led to conflicting conclusions depending on the system used (*in vitro*, transfected or transgenic substrates, engineered endogenous loci…). While some studies provided strong support to the notion that transcription was the pioneering factor for V(D)J recombination (e.g. (17–20)), others reported instances where V(D)J recombination took place in the absence of detectable transcription (e.g. (21–29)), or where transcribed V gene segments did not rearrange efficiently (e.g. (23,30–32)). Thus, whether transcription is the causal factor of accessibility or whether it is a by-product of other processes that generate accessibility is still unanswered.

The variable region of the mouse *IgH* locus contains 195 V_H genes followed by a dozen of D segments, and four J_H segments, followed by the constant region containing multiple constant genes (33,34). V(D)J recombination at the *IgH* locus occurs in two steps, first D-J_H recombination followed by V_H-DJ_H joining (35). The ordered rearrangement of the *IgH* gene segments is associated with various transcriptional events and chromatin modifications, and is controlled to a large extent by accessibility control elements, including enhancers, insulators and promoters, in a cell-type and developmental-stage specific manner (13,35,36). In particular, the Eμ enhancer, located immediately downstream of the *IgH* RC, plays a critical role in V(D)J recombination and associated germline transcription. Various deletion studies showed that Eμ controls sense and antisense transcription and D-J_H recombination within the ∼64 kb domain spanning the D and J_H segments (19,37–39). Specifically, Eμ is the key control element of the transcriptional, epigenetic and recombinational events that take place in the *IgH* RC (19,37–42), making it difficult to conclude if Eμ controls transcription and recombination in the RC through the same or different mechanisms.

Attempts to dissociate transcription and recombination within the *IgH* RC is tricky because, as mentioned above, the RC provides an optimal environment for both processes, and deletion of Eμ typically affects both transcription and recombination (19,37–39). We have previously adopted an alternative approach by inserting transcriptional insulators upstream of Eμ enhancer, leaving intact the enhancer (42). In particular, insertion of an imprinting control region (ICR) reduced transcription but not D–J_H recombination. Notably, the CpGs of the paternally-inherited ICR were methylated and led to a stronger effect on transcription than the maternally inherited, CTCF-binding ICR. But the occurrence of substantial transcription precluded a firm conclusion on the relationship between transcription and recombination in the RC (42). Nonetheless, this suggested to us that manipulating the methylation state and the density of CpGs could be a useful tool to dissociate transcription from recombination. Building on this, we generated a mouse line carrying a CpG-rich sequence and analysed the relationship between transcription and recombination.

We report data at the single cell level suggesting that the ectopic sequence promotes recombination in the RC in the absence of transcription. Chromatin remodeling in contrast is intact, and efficient D–J_H recombination correlates with RAG1 recruitment despite defective transcription-associated recruitment of RAG2.

MATERIALS AND METHODS

Mice

Experiments on mice were carried out according to CNRS ethical guidelines and were approved by the Midi-Pyrénées Regional Ethical Committee (Accreditation No. E31555005). The WT and homozygous $Rag2^{-/-}$, CGI-Eμ and CGI-Eμ/$Rag2^{-/-}$ mice were of 129Sv genetic background. All the mice used were 6–8 weeks old. Generation of CGI-Eμ mouse line is described in detail in Supplementary information.

Cell purification

Single cell suspensions from bone marrows were obtained by standard techniques. *Rag2*-deficient pro-B cells were positively sorted with B220- and CD19-magnetic microbeads and MS columns (Miltenyi). WT and CGI pro-B cells were sorted by flow cytometry as a $B220^{+}IgM^{-}CD43^{high}$ population, the purity of the pro-B cell populations was determined by FACS and the rearrangement status of *Igκ* locus.

Antibodies and cytokines

Allophycocyanin (APC)-conjugated anti-B220, APC-conjugated anti-CD19, Fluorescein isothiocyanate (FITC)-conjugated anti-IgM, and Phycoerythrin (PE)-conjugated anti-CD43 antibodies were purchased from BioLegend. FITC-conjugated anti-IgM^a and PE-conjugated anti-IgM^b were from BD-Pharmingen.

Fluorescence-activated cell sorting (FACS) analyses

Single-cell suspensions from bone marrows or spleens from 6- to 8-week-old mice were prepared by standard techniques. Cells (1×10^6 cells/assay) were stained and gated as indicated in figure legends. Data on 1×10^4 viable cells were obtained using a BD LSR Fortessa X-20 flow cytometer.

Primers

All the primers used in this study are listed in the Supplementary Table S1.

DNA methylation analyses

Purified genomic DNAs from sorted pro-B cells were assayed by sodium bisulphite sequencing by using a bisulphite conversion kit (Diagenode). Amplification of the modified templates, treatment of PCR products, and sequencing were as described (43). Bisulphite modification efficiency was checked by sequencing (99–100% efficiency).

V(D)J rearrangement assays

Genomic DNAs from WT and CGI-Eμ pro-B cells were prepared by standard techniques and diluted to 5 ng/μl

for the quantitative PCR (qPCR) assays (44). The fluorescence signals corresponding to the recombination products (DJ_H or V_HDJ_H) were normalized against the reference HS5 signals and are reported as percentage of WT. The histograms show the average of four recombination products.

Semi-quantitative PCR (semi-qPCR)

Total RNAs were extracted from sorted Rag2-deficient pro-B cells, reverse transcribed and subjected to PCR using Hot Start Taq polymerase (Ozyme). The cDNA samples were serial diluted 5-fold and run on a 2% agarose gel. The gel was colored with Syber Green I for 45 min and revealed with a Quantum gel imager (Vilber). Results were quantified by ImageJ software.

Reverse transcription-qPCR (RT-qPCR)

Total RNAs were prepared from WT, CGI-Eμ, $Rag2^{-/-}$ and CGI-Eμ/$Rag2^{-/-}$ pro-B cells, reverse transcribed (Invitrogen) and subjected to qPCR using Sso Fast Eva Green (BioRad). *Actin* transcripts were used for normalization.

Single cell RT-qPCR

Bone marrow B cells from two $Rag2^{-/-}$ or CGI-Eμ/$Rag2^{-/-}$ mice were stained with anti-B220 APC antibody. Individual $B220^+$ cells were then FACS sorted using a BD FACS Aria Fusion machine directly into 96-well PCR plates, reverse transcribed and subjected to qPCR as described previously (45).

Single-cell qPCR

Bone marrow B cells from three WT or CGI-Eμ mice were stained with anti-B220 APC, anti-CD43 PE and anti-IgM FITC antibodies and individual $B220^+IgM^-CD43^{high}$ cells were FACS sorted using a BD FACS Aria Fusion machine directly into 96-well PCR plates containing 1× Colorless Go Taq buffer (Promega), 0.5 mg/ml proteinase K, 10 μg/ml tRNA and water. The plates were then incubated at 55°C for 1 h, at 95°C for 10 min, and subjected to qPCR using Sso Fast Eva Green. Each plate was used to amplify a single $D–J_H$ rearrangement.

Chromatin immunoprecipitation (ChIP)

Chromatin was prepared from 5×10^6 *Rag2*-deficient pro-B cells. Chromatin was cross-linked for 10 min at RT with 1% formaldehyde, followed by quenching with 0.125 M glycine. Cross-linked chromatin was then lysed (0.5% SDS, 50 mM Tris, 10 mM EDTA, 1× PIC) and sonicated for 5–10 cycles 30 s ON–30 s OFF (Diagenode Bioruptor). Sonicated chromatin was diluted 10 times (0.01% SDS, 1.1% Triton X-100, 1.2 mM EDTA, 16.7 mM Tris–HCl, 167 mM NaCl) and precleared with 100 μl of Dynabeads protein-A magnetic beads (Invitrogen) and 5 μl of anti-IgG (Diagenode) for 2 h at 4°C. 5–10% of the precleared chromatin was used as the input sample. Immunoprecipitations were performed overnight at 4°C with 1×10^6 cells and 3 μg of anti-RNA polymerase II (Diagenode, C15200004), 3 μg of anti-RNA polymerase II CTD repeat YSPTSPS (phospho S5) (Abcam, ab5131), 3 μg of anti-RNA polymerase II CTD repeat YSPTSPS (phospho S2) (Abcam, ab24758), 3 μg anti-H3K4me3 (Diagenode, C15410003), 5 μl of anti-BRG1 (Merck, 07-478), 3 μg anti-RAG1 (Abcam, ab172637), 10 μl anti-CTCF (Merck, 07-729) or control anti-IgG (Diagenode, C15410206) per immunoprecipitation. Immunoprecipitated material was recovered with protein A magnetic beads (2 h at 4°C) and washed. Crosslinking was reversed overnight at 45°C. Eluted DNA was extracted by standard techniques and subjected to qPCR. Results are presented as fold enrichment, taking into account both the input and the negative (IgG) sample.

Statistical analysis

Results are expressed as mean ± SD (GraphPad Prism), and overall differences between values were evaluated by a two-tailed paired (for V(D)J recombination and germline transcription studies) or unpaired (for all the other experiments) *t*-test. The difference between means is not significant (ns) or significant if P value < 0.05 (*), very significant if P value < 0.01 (**), extremely significant if P value < 0.001 (***) and P value < 0.0001 (****).

RESULTS

We generated a mouse line carrying a CpG-rich sequence (hereafter CGI sequence), derived from the bacteriophage λ, between J_{H4} and Eμ enhancer (Supplementary Figure S1) (hereafter CGI-Eμ line). Preliminary experiments on germline transcription in the *IgH* RC revealed a strong reduction in the levels of transcripts derived from D_{Q52} promoter despite a surprisingly robust $D_{Q52}–J_H$ recombination, the CGI-Eμ mouse line was therefore selected for further analyses described in detail below and in the Supplementary information. Unless otherwise indicated, all experiments were performed on homozygous mice.

Insertion of a CGI sequence upstream of Eμ enhancer moderately affects DNA methylation in the recombination centre

Analysis of DNA methylation within the D_{Q52}-Eμ region revealed that, prior to V(D)J recombination, J_H segments were partially methylated while the Eμ and D_{Q52} regions were un-methylated (41). The phage λ-derived 2565 bp-long CGI insert contains 217 CpGs (and 496 Cs and 547 Gs outside the CpGs). Given the origin and the content of the CGI sequence (46), and because it was transmitted through the germline, it was important to determine the methylation state of the insert and check if the insertion perturbed the methylation profile of the flanking un-rearranged segments. This issue was addressed by using bisulphite sequencing in RAG2-deficient background which prevents V(D)J recombination.

We found that the ectopic sequence was essentially unmethylated except for the most distal CpGs, which showed low levels of methylation (Figure 1). The un-methylated pattern of CGI was maintained in splenic B cells (not shown).

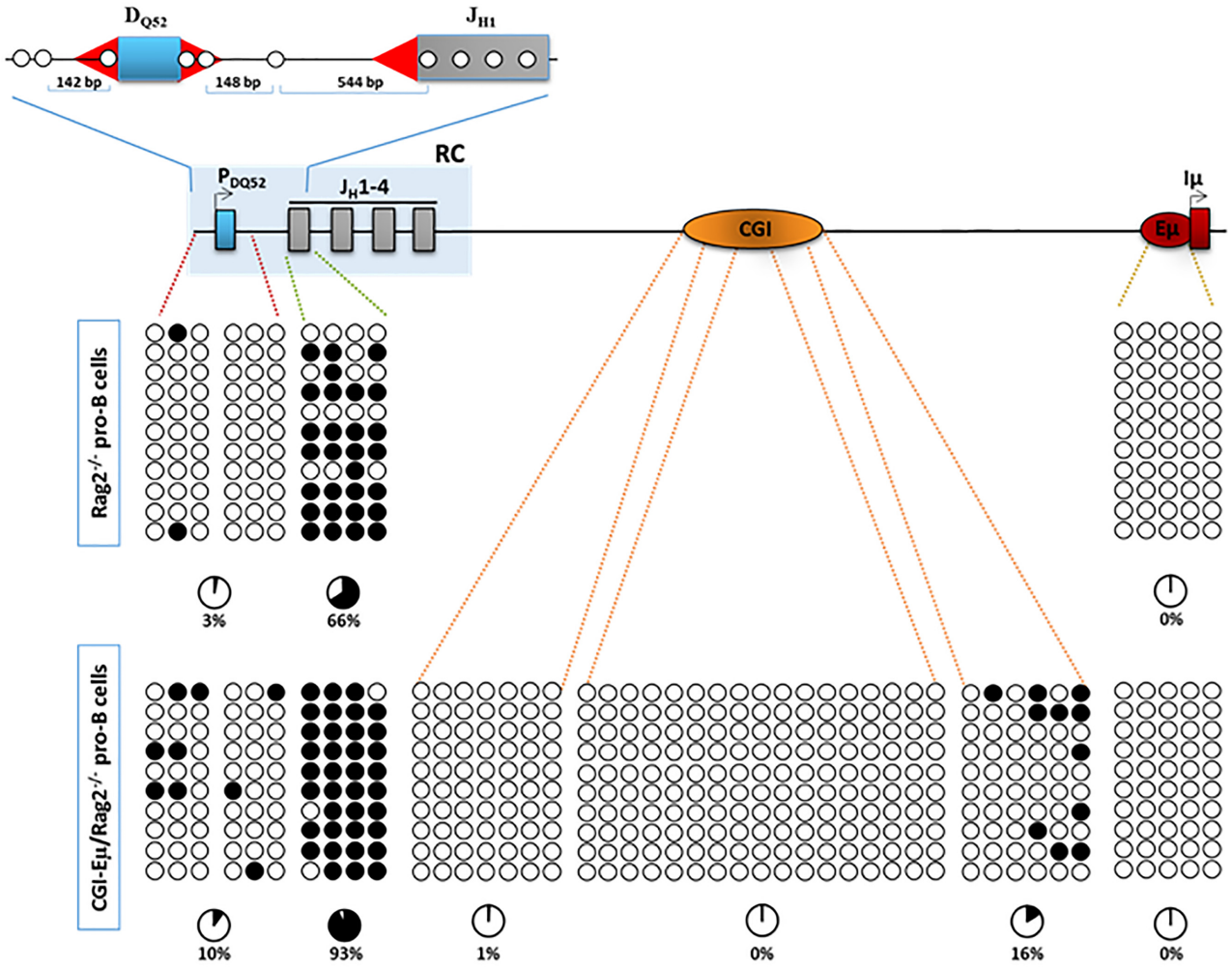

Figure 1. DNA methylation profiles in the recombination centre. The *IgH* RC is ∼2.5 kb long and contains the most 3′ D segment, D_{Q52}, at ∼700 bp from the J_H region spread over ∼1.4 kb. The RC is followed by the Eμ enhancer at ∼600 bp from J_{H4}. CpG methylation of D_{Q52}, J_{H1}, CGI and the core Eμ were assayed by bisulphite sequencing. For the ectopic CGI, CpG methylation was determined at the 5′, middle and 3′ parts of the insert. The D_{Q52}-J_{H1} region is highlighted in the top scheme. Of the six CpGs analysed in the of D_{Q52} region, the two 5′ CpGs are located within D_{Q52} promoter region, the third CpG at the 5′RSS (in red) of D_{Q52} segment. The fourth and the fifth CpGs are located within the 3′RSS of D_{Q52} (in red). The sixth is 544 bp away from the first CpG of J_{H1} segment (the 544 bp sequence contains two CpGs not sequenced and not shown here). Horizontal lines indicate the number and the methylation status of sequenced CpGs and vertical lines, the number of sequenced independent clones. The un-methylated and methylated cytosines are represented by open and filled circles, respectively. The results are summarized in the form of pie charts and the percentage of methylated residues is indicated underneath the indicated elements.

Consistent with previous findings (41), the Eμ and D_{Q52} regions were un-methylated in Rag2$^{-/-}$ pro-B cells, and were also un-methylated in CGI-Eμ/Rag2$^{-/-}$ pro-B cells (Figure 1). In particular, the two most upstream CpGs located in D_{Q52} promoter region and the third CpG located in the 5′ RSS of D_{Q52} segment did not undergo significant methylation in CGI-Eμ/Rag2$^{-/-}$ pro-B cells (Figure 1). In contrast, J_{H1} segment was hyper-methylated in CGI-Eμ/Rag2$^{-/-}$ compared to the partially methylated J_{H1} in Rag2$^{-/-}$ pro-B cells, especially for the two central CpGs, which were fully methylated (Figure 1).

Thus, the CGI sequence was essentially un-methylated when inserted upstream of the Eμ enhancer, and while it promoted further methylation of J_{H1} segment, it did not perturb the un-methylated pattern of Eμ enhancer and the unrearranged D_{Q52} region.

Ectopic CGI promotes an accumulation of DJ_H intermediates despite strongly reduced transcription

To investigate the effect of CGI insertion on D–J_H recombination, we used a qPCR assay to quantify rearranged DJ_H segments in purified pro-B cells (B220$^+$CD43^{high}IgM$^-$) (44). Although the focus of this study was the relationship between transcription and recombination in the RC, we extended our analyses to the upstream D_{SP} family. A degenerate forward primer that anneals upstream of D_{SP} segments, a specific forward primer that anneals upstream of the unique D_{Q52} segment, and specific reverse primers that anneal downstream of J_H segments were used to amplify DJ_H intermediates.

With the exception of $D_{SP}J_{H4}$ segments whose frequency did not significantly vary, there was in the mean a ∼1.7-fold accumulation of rearranged $D_{SP}J_H$ alleles (i.e. including all

J_H segments) in CGI-Eμ pro-B cells (Figure 2A). $D_{Q52}J_{H3}$ and $D_{Q52}J_{H4}$ on the mutant alleles occurred at similar frequency as their WT counterparts. In contrast, there was ∼7-fold more $D_{Q52}J_{H1}$ and $D_{Q52}J_{H2}$ on the mutant alleles. By including all J_H segments, there was in average ∼4 times more $D_{Q52}J_H$ mutant alleles (Figure 2A). We could not detect a single instance where DJ_H mutant alleles were lower than WT controls (not shown). We conclude that CGI insertion resulted in an overall accumulation of DJ_H intermediates.

To determine how the accumulation of DJ_H alleles correlated with germline transcription, we quantified the transcript levels of un-rearranged segments within the D–Cμ domain, which includes Iμ sense transcripts derived from Eμ/Iμ enhancer/promoter, μ0 sense transcripts derived from D_{Q52} promoter, and anti-sense transcripts that initiate within the J_{H4}-Eμ region.

We found no significant difference in Iμ transcript levels (Figure 2B). In contrast, there was a ∼4-fold drop in D_{SP} transcript levels in CGI-Eμ/Rag2$^{-/-}$ pro-B cells. The decrease was stronger for μ0 transcript levels (∼13-fold decrease) (Figure 2B), and was associated with only a moderate reduction in μ0 transcripts' half-lives (Supplementary Figure S2).

We conclude that within the D-Cμ domain, the ectopic CGI promoted an accumulation of DJ_H segments despite severely reduced germline transcription.

D–J_H recombination may occur in the absence of detectable transcription

Two possible scenarios may account for the unexpected finding that D–J_H recombination occurred efficiently despite strong reduction of germline transcription. It is conceivable that very low levels of transcription across the RSSs were sufficient to initiate recombination within the D–Cμ domain. Alternatively, recombination could occur in a fraction of the population in the absence of detectable transcription. Because it is difficult to provide a straightforward evidence for or against each scenario when dealing with pro-B cell populations, we attempted a single-cell approach. We reasoned that by scoring the total recombination events and correlating these to the total number of single cells that produced either μ0, D_{SP} or both transcripts, we could draw a reliable correlation between recombination and transcription. By force, this approach enables only correlations as germline transcription is assayed in Rag-deficient background whereas D–J_H recombination is assayed in Rag-proficient background (see discussion).

To address the correlation between transcription and recombination, Rag2-deficient and Rag2-proficient pro-B cells were single-sorted and assayed for transcription and D-J_H recombination respectively. The RT-qPCR was performed by using three sets of primer pairs that amplify Iμ, μ0 and D_{SP} transcripts. Of the total Iμ$^+$ single cells, we found that ∼50% of CGI-Eμ/Rag2$^{-/-}$ single cells produced neither μ0 nor D_{SP} transcripts (i.e. Iμ$^+$μ0$^-$$D_{SP}^-$), whereas only ∼6% of Rag2$^{-/-}$ single cells were μ0$^-$$D_{SP}^-$ (∼8-fold increase) (Figure 3A). About 9% were μ0$^+$$D_{SP}^+$ compared to ∼50% in Rag2$^{-/-}$ control (∼5-fold decrease) (Figure 3B). Among the producers, the levels of Iμ, μ0 and D_{SP} transcripts were comparable between CGI-Eμ/Rag2$^{-/-}$ and Rag2$^{-/-}$pro-B cells (not shown), suggesting that the decrease in μ0 and D_{SP} transcript levels seen at the level of CGI-Eμ/Rag2$^{-/-}$ pro-B cell population (Figure 2B) was due to a reduction in the number of single cells that transcribe.

Taking into account both single (μ0$^-$$D_{SP}^+$) and double-producers (μ0$^+$$D_{SP}^+$), 29% of CGI-Eμ/Rag2$^{-/-}$ single cells were D_{SP}^+ compared to 61% in Rag2$^{-/-}$ controls (∼2-fold decrease) (Figure 3C). However, when we looked at the number of recombined alleles, we found that 47% of total CGI-Eμ alleles were $D_{SP}J_H$ alleles compared to 51% of WT $D_{SP}J_H$ alleles (Figure 3D). More revealing, in the RC, while 32% of CGI-Eμ/Rag2$^{-/-}$ single cells were μ0$^+$ (including μ0$^+$$D_{SP}^-$ and μ0$^+$$D_{SP}^+$) compared to 82% in Rag2$^{-/-}$ controls (∼2.5-fold decrease) (Figure 3E), there was a ∼1.4-fold increase in the number of CGI-Eμ alleles that underwent D_{Q52}–J_H rearrangements (Figure 3F).

The simplest explanation of the above figures is that a fraction of the CGI-Eμ pro-B cell population underwent D–J_H recombination without having transcribed. Thus, within the D–Cμ domain, the CGI insertion promoted recombination in the absence of detectable transcription.

Efficient recruitment of RAG1 and BRG1 in the recombination centre despite reduced transcription

The data on D-J_H recombination strongly suggested that the RSSs of D and J_H segments on the CGI-Eμ alleles were accessible to the RAG recombinase. To investigate how accessibility was achieved in RC despite reduced transcriptional elongation across the RSSs, we performed chromatin immunoprecipitation (ChIP) assays on factors known to be important for transcription and D-J_H recombination.

As expected, RNAp II, RNAp II CTD-S5 and RNAp II CTD-S2 density at Eμ enhancer was comparable on mutant and WT alleles. Consistent with reduced transcription, there was a significant decrease in RNAp II at D_{SP}, D_{Q52} and J_{H4} segments in CGI-Eμ/Rag2$^{-/-}$ pro-B cells (Figure 4). Accordingly, both RNAp II CTD-S5 and RNAp II CTD-S2 were diminished (Figure 4), confirming that the insertion affected initiation and elongation of transcription at these segments.

The H3K4me3 mark is associated with transcriptional activation and is enriched in promoter regions and the proximal part of transcription units (47), and binds the PHD finger of RAG2 (6,7). Besides the D_{SP} segments, known to be depleted in H3K4me3 (9,39,40), we detected a decrease in this mark in the RC of CGI-Eμ/Rag2$^{-/-}$ pro-B cells (Figure 4). As ChIP experiments were performed in Rag2-deficient background, we did not perform ChIP assay on RAG2 subunit. Nonetheless, because of the strong correlation between RAG2 recruitment and H3K4me3 mark (9), we assume that a reduction in H3K4me3 deposition in the RC reflects reduced recruitment of RAG2.

Interestingly, binding of RAG1 was detected in the RC and was comparable between CGI-Eμ/Rag2$^{-/-}$ pro-B cells and Rag2$^{-/-}$ controls (Figure 4). Unexpectedly, relatively high levels of binding were found at the D_{SP} region and were also comparable between CGI-Eμ/Rag2$^{-/-}$ and Rag2$^{-/-}$ pro-B cells (Figure 4), suggesting that RAG1 got access to

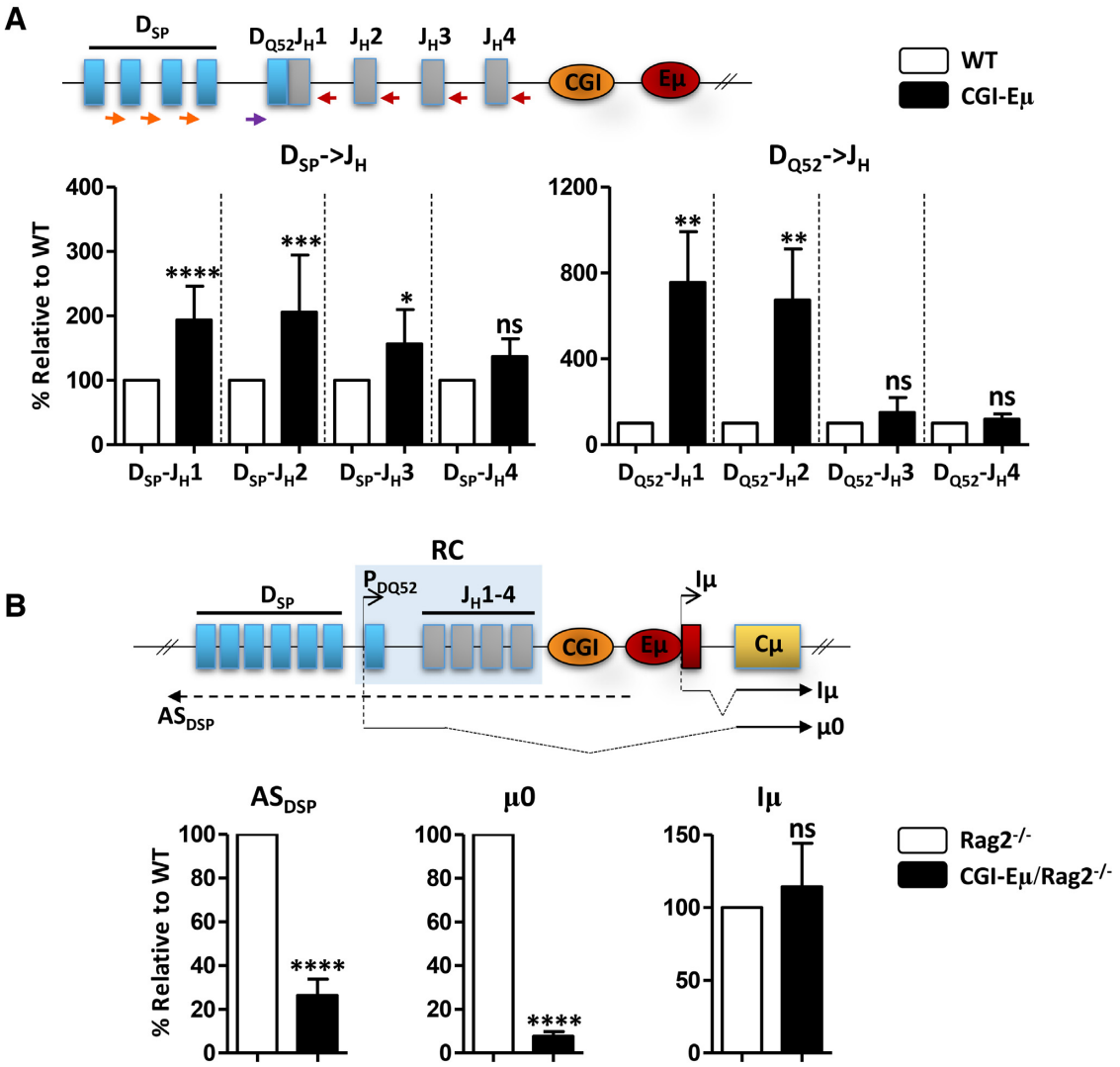

Figure 2. Analysis of D–J_H recombination and germline transcription. (**A**) The top scheme represents an example of D-J_H rearrangement involving D_{Q52} and J_{H1} segments. The arrows represent the primers used to amplify DJ_H recombination intermediates. The D_{Q52} forward primer and the J_H reverse primers are specific whereas D_{SP} forward primer is degenerate. Genomic DNA from sorted WT and CGI-Eμ pro-B cells was extracted and subjected to qPCR to amplify D_{SP}-J_H and D_{Q52}-J_H rearrangements. WT genomic recombination levels were set to 100%. The DNaseI hypersensitive site HS5 located downstream of the *IgH* locus was used for normalization. The histograms show the standard deviation ($n \geq 4$). (**B**) The top scheme outlines the three germline transcripts produced within the D-Cμ domain. μ0 and Iμ sense transcripts derived from the D_{Q52} and Iμ germline promoters, respectively; D_{SP} antisense transcripts that initiate at the Eμ region run across the J_H and D segments. Dots indicate that the initiation and termination sites of AS_{DSP} transcripts have not been mapped precisely. Total RNAs from sorted Rag2-deficient pro-B cells were extracted, reverse transcribed and subjected to qPCR for the indicated transcripts. The corresponding transcript levels in $Rag2^{-/-}$ controls were set to 100%. *Actin* transcripts were used for normalization. (-RT) control were included throughout. The histograms show the standard deviation (n≥6). Statistical analysis (*t*-test). (ns) not significant, (*) significant ($P < 0.05$), (**) very significant ($P < 0.01$), (***) and (****): extremely significant ($P < 0.001$ and $P < 0.0001$ respectively).

the RSSs of the D–J_H domain despite low transcriptional activity and absence of RAG2.

Chromatin remodeling provides an alternative mechanism for RSS accessibility in the absence of transcription (29) (see Discussion). BRG1, the catalytic subunit of the chromatin remodeling complex SWI/SNF, was shown to bind the *IgH* D–J_H region (48). This led us to investigate how reduced transcription in the D–J_H domain of CGI-Eμ/$Rag2^{-/-}$ pro-B cells correlated with BRG1 recruitment. We found that the levels of BRG1 bound to D_{SP} and J_H regions were comparable between CGI-Eμ/$Rag2^{-/-}$ pro-B cells and $Rag2^{-/-}$ controls (Figure 4). In contrast, relatively higher binding of BRG1 to D_{Q52} chromatin was detected in CGI-Eμ/$Rag2^{-/-}$ pro-B cells (Figure 4).

Altogether, the data showed that reduced transcriptional elongation across the CGI-Eμ RSSs within the D–J_H domain was associated with a decrease of H3K4me3 mark, and that RAG1 and the SWI/SNF subunit BRG1 were efficiently recruited.

CGI insertion impairs V_H–DJ recombination

The observed accumulation of DJ_H alleles in CGI-Eμ pro-B cells raises the question as to the effect of the mu-

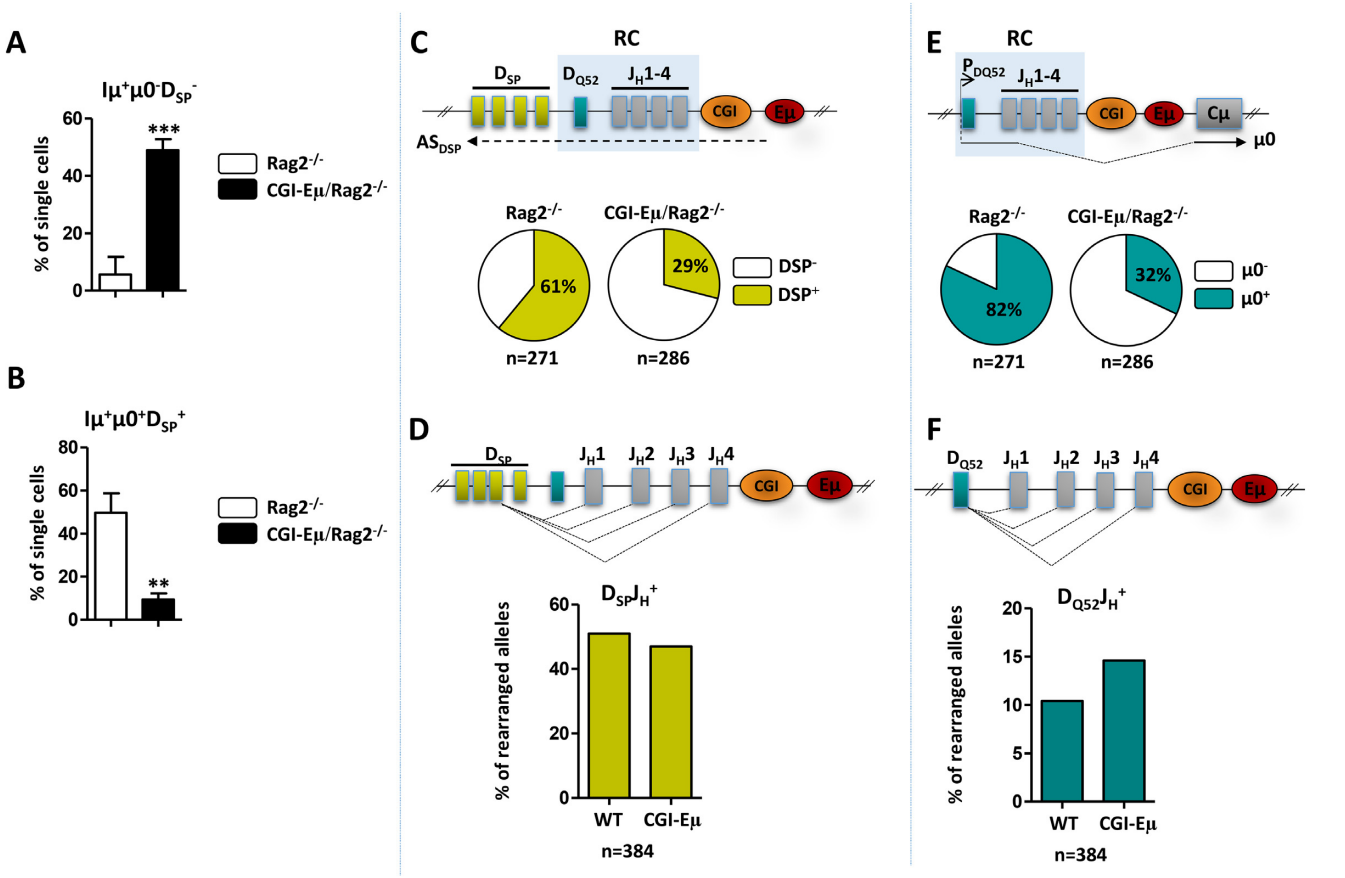

Figure 3. Single-cell analysis of germline transcription and D-J_H recombination. (**A**) Percentage of single cells that produced Iμ transcripts exclusively ($I\mu^+\mu0^-DSP^-$). (**B**) Percentage of single cells that produced the three sets of transcripts ($I\mu^+\mu0^+DSP^+$). (**C**) Percentage of D_{SP} transcript-producing cells upon single-cell RT-qPCR. The D_{SP} anti-sense (AS) transcript is indicated in the upper scheme. Total RNA from single-sorted pro-B cells from two $Rag2^{-/-}$ and CGI-Eμ/$Rag2^{-/-}$ mice were assayed by RT-qPCR for the indicated transcript (*n* indicates the number of $I\mu^+$ single cells analysed). Note that total D_{SP}^+ cells include both $\mu0^+$ and $\mu0^-$ cells. (**D**) The histograms represent the percentage of $D_{SP}J_H$ alleles. Genomic DNAs from single-sorted pro-B cells from a pool of two WT and two CGI-Eμ mice were extracted and assayed for D_{SP}-J_H rearrangements, and from a pool of twelve WT and seven CGI-Eμ mice for D_{Q52}-J_H rearrangements. HS5 was used as a control. (**E**) μ0 transcript-expressing cells upon single-cell RT-qPCR, with the upper scheme representing the corresponding μ0 spliced sense transcript. Note that total $\mu0^+$ cells include both D_{SP}^+ and D_{SP}^- cells. Total RNAs were prepared as in (C). (**F**) Percentage of WT and CGI-Eμ D_{Q52}-J_H alleles. Genomic DNAs were prepared as in (D). Statistical analysis (*t*-test). (**): very significant ($P < 0.01$), (***): extremely significant ($P < 0.001$).

tation on V_H–DJ_H recombination. Previous studies suggested that in Eμ-deficient alleles, defective V_H–DJ_H was a downstream consequence of the primary block in D-J_H recombination (38), while we found that alleles bearing transcriptional insulators upstream of Eμ had defective V_H–DJ_H recombination despite accumulated DJ_H intermediates (42). To investigate the effect of CGI insertion on V_H recombination, pro-B cells from the bone marrows of WT and CGI-Eμ mice were sorted and their genomic DNAs were assayed for V_H–DJ_H recombination by qPCR.

V_H-DJ_H recombination involving distal V_H segments was reduced by half in CGI-Eμ pro-B cells regardless of the DJ_H segment. The reduction was relatively more severe for the proximal V_H segments including the V_{H81X} (4–5-fold decrease) (Figure 5A). To investigate if this reduction correlated with reduced germline transcription, we quantified anti-sense transcript levels in the distal and proximal V_H domains by focusing on intergenic regions (17). Anti-sense transcript levels in the proximal domain of CGI-Eμ/$Rag2^{-/-}$ pro-B cells were comparable to their $Rag2^{-/-}$ counterparts. This was true by using a primer pair that annealed at multiple sites within the proximal domain or a specific pair that annealed at one site upstream of the V_{H81X} gene segment (Figure 5B). The levels of anti-sense transcripts within the distal V_H domain were reduced (Figure 5B). We also checked by semi-quantitative PCR that this reduction involved both the spliced (sense) and the unspliced (including primary sense and anti-sense) transcripts (Figure 5C). In contrast, anti-sense transcripts levels corresponding to the distal PAIR4 and the middle domain V_{HJ606} family were slightly increased (Figure 5B).

Thus, CGI insertion affected V_H–DJ_H recombination, and while reduced V_{HJ558}–DJ_H recombination correlated with reduced germline transcription within the distal J558 domain, the correlation did not stand for the proximal and the middle domains.

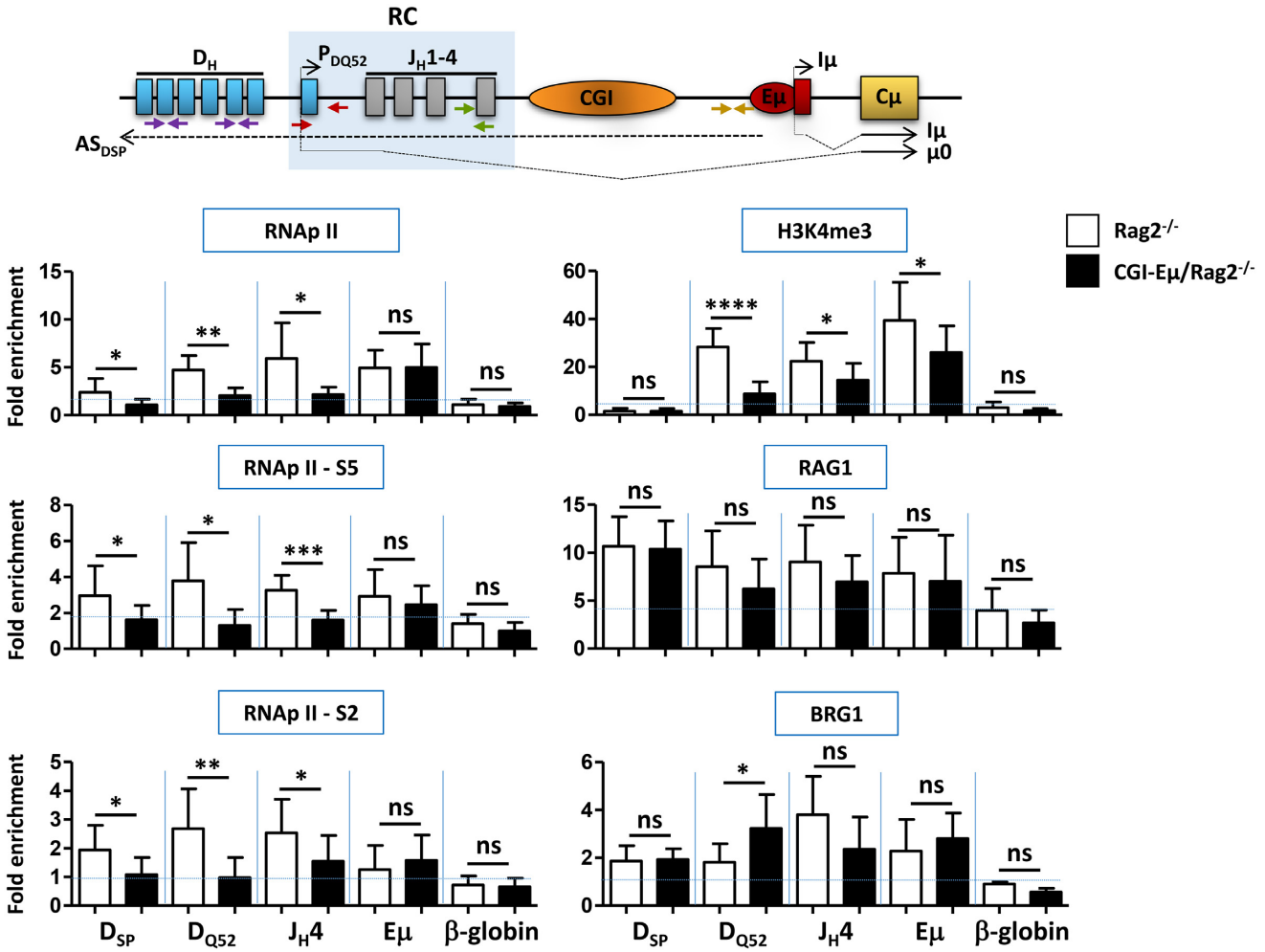

Figure 4. ChIP on factors involved in D–J_H recombination. The D–Cμ domain in its unrearranged configuration is shown in the top scheme together with the sense and anti-sense transcripts (black arrows) produced in the domain. The relative position of the primers (colored arrows) used in qPCR is indicated. Degenerate primers were used to amplify D_{SP} segments. The histograms below show the fold enrichment for RNA polymerase II and its phosphorylated forms at Serine 5 (S5) or at Serine 2 (S2), H3K4me3, RAG1 and the BRG1 subunit of the SWI/SNF remodeling complex. Chromatin from Rag2-deficient pro-B cells was immunoprecipitated with the corresponding antibodies. The β-globin gene was used as a negative control. The histograms show the standard deviation ($n \geq 5$). Statistical analysis (*t*-test). (ns): not significant, (*) significant ($P < 0.05$), (**) very significant ($P < 0.01$), (***) and (****): extremely significant ($P < 0.001$ and $P < 0.0001$ respectively).

CGI insertion inhibits transcription of rearranged alleles and perturbs the demethylating activity of Eμ enhancer

We have previously shown that DJ_H (also called Dμ) transcription was critical for efficient V_H–DJ_H recombination (42). DJ_H transcription initiates from the promoter of the rearranged D segment and terminates downstream of the Cμ constant region (49,50). We quantified DJ_H transcript levels and found that in CGI-Eμ pro-B cells, there was no detectable DJ_H transcription, regardless of the recombined D segment (Figure 6A).

To investigate how inhibition of DJ_H transcription correlated with DNA methylation in the DJ RC, we analysed CpG methylation of recombined $D_{Q52}J_{H1}$ segments. It was previously shown that demethylation of recombined J_H segments was Eμ-dependent (41). Accordingly, we found that the J_{H1} segment on WT alleles became un-methylated upon D–J_H recombination (Figure 6B). Interestingly, the recombined J_{H1} segment on the CGI-Eμ alleles was fully methylated (Figure 6B) suggesting that the CGI insertion inhibited the Eμ-dependent demethylation of the recombined J_{H1}. Additionally, the CpG at the RSS of $D_{Q52}J_{H1}$ segment, which was hypomethylated before D_{Q52} recombination (Figure 1), became heavily methylated upon recombination (Figure 6B). Hypermethylation of $D_{Q52}J_{H1}$ RSS was highly focused because the two more upstream CpGs (~140 bp upstream of the RSS, see Figure 1), located in D_{Q52} promoter region, remained hypomethylated (Figure 6B).

Thus, CGI insertion upstream of Eμ enhancer inhibited DJ_H transcription. This inhibition correlated with a failure to demethylate J_H segments, and at least for the rearranged $D_{Q52}J_{H1}$ segments, was associated with hypermethylation of the RSS, suggesting that Eμ demethylating activity was compromised. In contrast, D_{Q52} promoter region remained hypomethylated.

The complete shutdown of DJ_H transcription led us to ask if inhibition of transcription persisted after completion

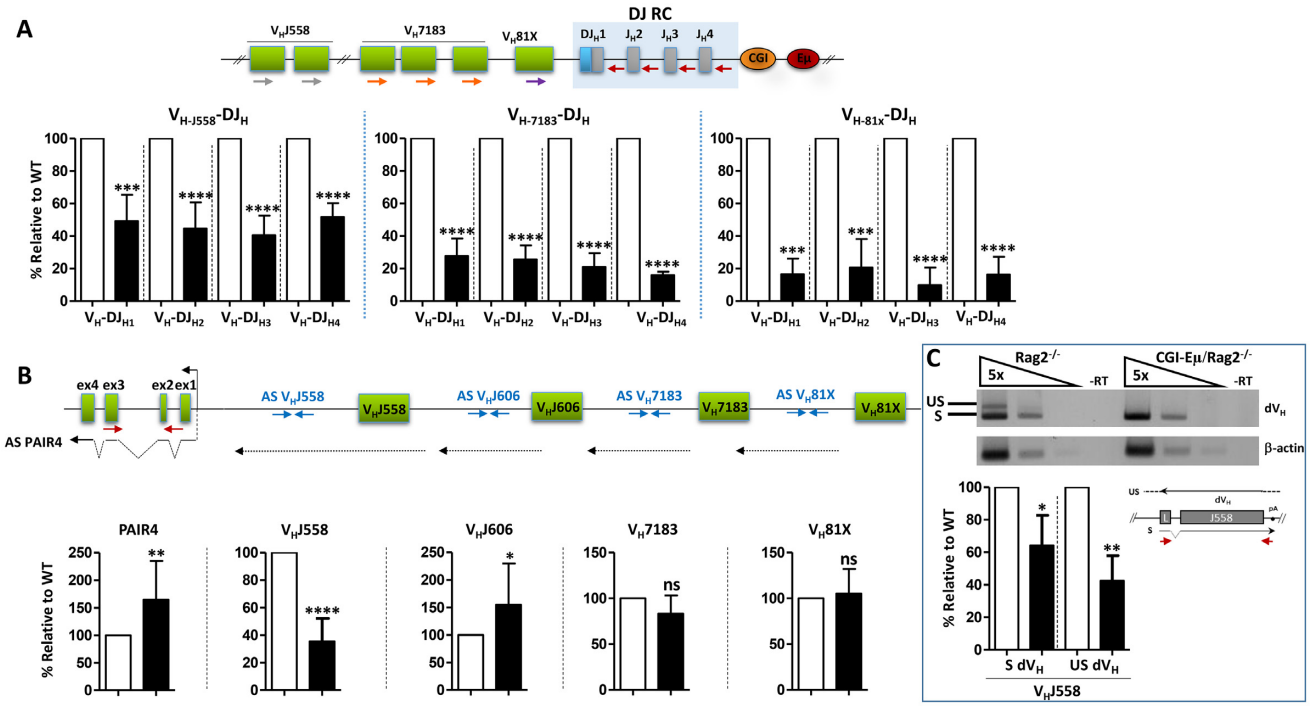

Figure 5. V_H–DJ_H recombination and germline transcription in the V_H region. (**A**) V_H–DJ_H recombination is impaired in CGI-Eμ pro-B cells. The upper scheme represents a partially rearranged DJ allele and the newly formed DJ RC. The relative position of the primers (colored arrows) used for V_H–DJ_H recombination assay is indicated. Forward degenerate primers anneal to multiple V_H segments within each family, whereas J_H reverse primers are specific to each J_H segment. Genomic DNAs were prepared from WT and CGI-Eμ pro-B cells and subjected to qPCR. The histograms show the standard deviation ($n \geq 4$). WT recombination levels were set to 100%. (**B**) Lack of correlation between V_H germline transcription and V_H–DJ_H recombination. The top scheme shows the germline configuration of the V_H region (not to scale), including proximal and distal gene families, and the associated intergenic, anti-sense transcripts analyzed. The blue arrows represent the primers used to amplify intergenic transcripts. The red arrows indicate the primers used to amplify the spliced form of PAIR4 transcripts. Total RNAs from Rag2-deficient pro-B cells were assayed by RT-qPCR for the indicated transcripts. The signals of the corresponding transcripts in the *Rag2*$^{-/-}$ controls were set to 100%. The histograms show the standard deviation. *Actin* transcripts were used for normalization. (-RT) controls were included throughout ($n \geq 3$). (**C**) Defective germline transcription of $V_{H\text{-}J558}$ genes. Total RNAs were prepared as in (B) and assayed by semi-quantitative PCR ($n \geq 5$) for germline transcription across the distal $V_{H\text{-}J558}$ genes. *Actin* transcripts were used for normalization. One sample from each genotype is shown as an example. -RT, no reverse transcription. The histograms recapitulate the levels of spliced (sense) an unspliced (antisense and primary sense) $V_{H\text{-}J558}$ transcripts. The scheme on the right indicates the transcripts detected by semi-quantitative RT-qPCR assay and the relative position of the primers. L, leader; S, spliced; US, unspliced. Statistical analysis (*t*-test). (ns): not significant, (*) significant ($P < 0.05$), (**) very significant ($P < 0.01$), (***) and (****) extremely significant ($P < 0.001$ and $P < 0.0001$ respectively).

of V_H–DJ_H recombination. Indeed, though reduced, there was still substantial V_H-DJ_H recombination, which contrasted with the severe drop in CGI-Eμ pre-B and immature B cell populations (Supplementary Figure S3), and the inability of mutant allele to produce surface IgM when put in competition with the WT allele (Supplementary Figure S3). We found that V_HDJ_H transcription was abrogated in mutant pro-B cells, for all the V_H gene families tested (Figure 6C).

DISCUSSION

Transcription *versus* recombination in the *IgH* recombination centre

V(D)J recombination is a complex process that involves multiple layers of regulation including regulation of transcription, epigenetic modifications, nuclear localization and large-scale architectural reorganization of antigen receptor loci (2,11,13,14). Specifically, since the initial proposal of the accessibility model (16), various studies highlighted the role of transcription as a correlate of RSS accessibility (see Introduction). Within the V_H domain, it is now established that transcription is not sufficient for efficient V_H–DJ_H recombination, and that additional processes are required, in particular looping/contraction of the locus that brings the distant V_H gene segments close to the assembled DJ_H segments (2,11,13,14,51). By contrast, in the endogenous RC featuring close proximity between the J_H segments and the frequently recombining D_{Q52} segment (52–54) and optimal transcriptional and epigenetic landscape (see Introduction), a dissociation between transcription and recombination is more difficult to achieve.

In this study, we found at the single-cell level that a fraction of the CGI-Eμ pro-B cells underwent D–J_H recombination in the absence of detectable transcription within the D–J_H domain generally, and within the RC specifically. Nonetheless, the single-cell assay raises several issues. The fact that transcription and recombination were assayed in *Rag*-deficient and *Rag*-proficient backgrounds respectively has already been noted. Additionally, we cannot ascertain if a recombination event (e.g. D_{Q52}–J_{H1}) has taken place in a cell that produced μ0 transcript only or both μ0 and D_{SP} transcripts. Moreover, D-J_H recombination occurs on both alleles and can involve different D and J_H segments, for ex-

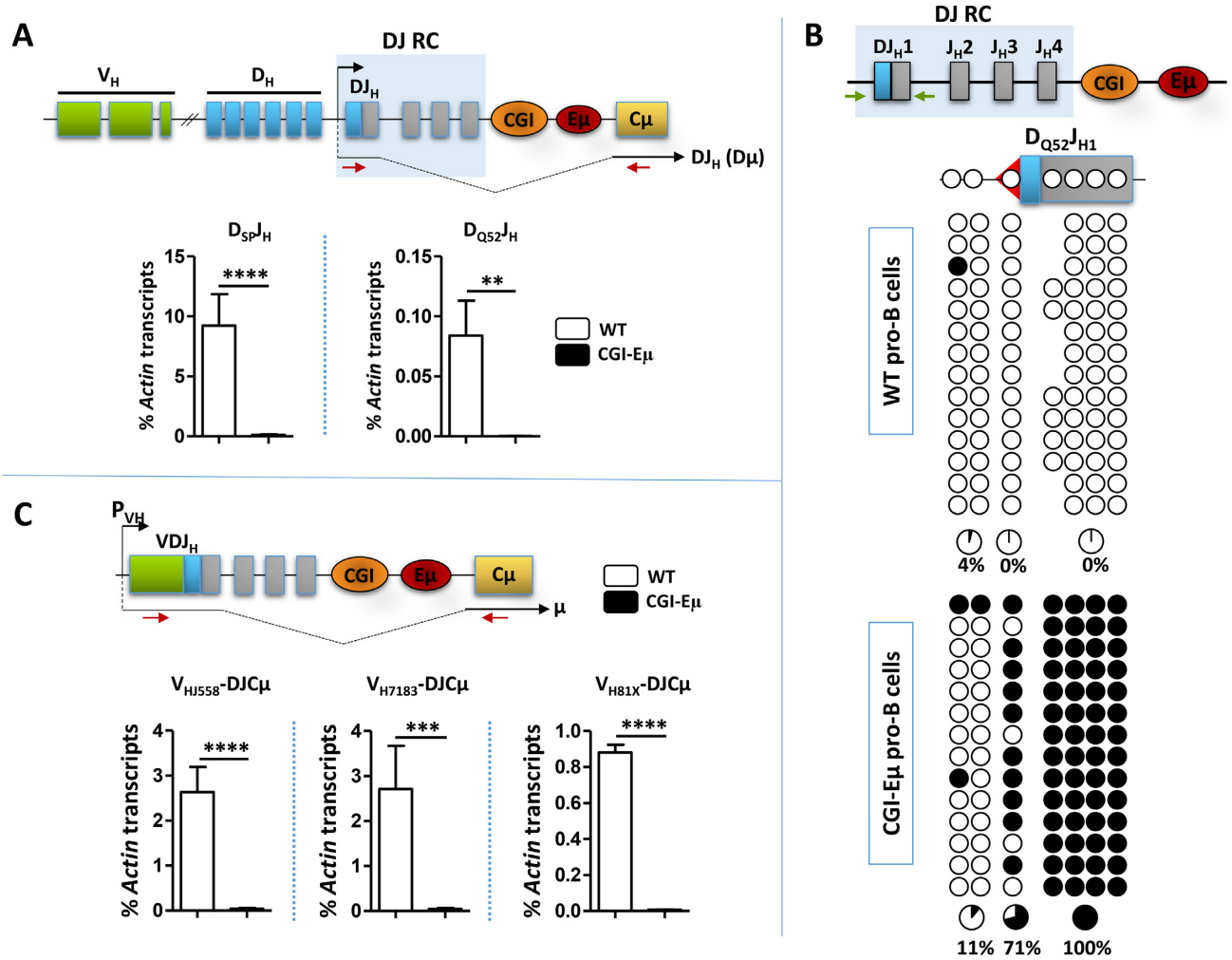

Figure 6. Transcription and DNA methylation are altered on rearranged mutant alleles. (**A**) The top scheme shows a partially rearranged DJ_H allele and the resulting DJ_H (also called Dμ) spliced transcript as well as the DJ RC. The primers used are shown as red arrows and the transcription start site by a black arrow. Total RNAs from WT and CGI-Eμ pro-B cells were extracted and reverse transcribed. Spliced DJ_H transcripts were quantified by qPCR. *Actin* transcripts were used for normalization. The histograms show the standard deviation ($n \geq 3$). (**B**) DNA methylation profiles of $D_{Q52}J_{H1}$ intermediates. CpG methylation was assayed by bisulphite sequencing. Note that the CpG at the 5′RSS (red triangle in the scheme) is heavily methylated and the J_{H1} CpGs are fully methylated on the CGI-Eμ allele. (**C**) The top scheme shows a fully rearranged gene and the resulting VDJ-Cμ transcript derived from the promoter (P_{VH}) of the recombined V_H gene segment. Red arrows indicate the localization of the primers and the black arrow, the transcription start site. Total RNAs from WT and CGI-Eμ pro-B cells were extracted and reverse transcribed. Spliced VDJ-Cμ transcripts involving distal and proximal V_H exons were quantified by qPCR. *Actin* transcripts were used for normalization. The histograms show the standard deviation (n≥3). Statistical analysis (*t*-test). (**) very significant ($P < 0.01$), (***) and (****) extremely significant ($P < 0.001$ and $P < 0.0001$ respectively).

ample D_{Q52} on one allele and one D_{SP} segment on the other allele can recombine with identical or different J_H segments. Hence, the assay provides strong correlations rather than direct evidence. Nonetheless, in view of the figures that we obtained with CGI-Eμ pro-B cells, i.e. the low number of transcribing cells relative to the high number of rearranging cells, and though we cannot provide absolute values, we can reasonably conclude that within the D–J_H domain, transcription is not always a prerequisite for recombination. This conclusion is consistent with the notion that Eμ enhancer, the key control element of transcription and recombination in the RC, directs the two processes through distinct mechanisms. Nonetheless, our findings do not formally exclude a more complex scenario whereby transcription could have occurred in a transient or stochastic manner, this would have allowed a low rate of D–J_H recombination which accumulated with time due to defective V_H–DJ_H recombination and differentiation.

The Eμ enhancer binds several transcription factors and co-activators (55), but the precise motifs involved in the control of transcription *versus* recombination are still unknown. By using transgenic substrates carrying various deletions of Eμ enhancer, it was suggested that a compound E-box motif containing μE1 (which binds YY1 transcription factor), and μE2 and μE5 (which bind the helix-loop-helix factor E2A) was likely required for the recombinational function of Eμ (31). However, B cell-specific ablation of YY1 had no effect on D-J_H recombination (56), suggesting that μE1 was not involved in the recombinational function of Eμ. On the other hand, deletion of E2A gene pre-

vented D-J_H initiation (57,58) but targeted deletion of E2A binding motifs at Eμ has not been attempted, though a cooperation between μE motifs (59) cannot be excluded.

Chromatin remodeling and RAG access to RSSs

An important question that arises is how RAG gets access to the RSSs in the CGI-Eμ RC despite defective germline transcription and associated RAG2 recruitment, at least as measured by reduced H3K4me3 density. Previous work showed that RAG1 and RAG2 can be independently recruited to the RCs of antigen receptor loci with the notable exception of the *IgH* RC where RAG1 binding was found to depend on the presence of RAG2 (9). We found that RAG1 got access to the *IgH* RC independently of RAG2 and of actively transcribed chromatin. The reasons underlying this discrepancy are unclear and may be due to the different ChIP assays. Although we cannot ascertain if the whole pool of RAG1, or only a fraction of it, bound first, our findings point to alternative mechanisms of RAG1 recruitment and specifically to the importance of chromatin remodeling.

At the endogenous *Tcrb* and *IgH* loci, recruitment of chromatin remodeling complexes for D-J recombination depends on the RC-proximal Eβ and Eμ enhancers respectively (60–62). *In vitro*, by using chromatinized recombination substrates, the chromatin remodeling complex SWI/SNF was sufficient to confer, through local chromatin alteration, accessibility to the RAG complex independently of transcription (29). At the endogenous *Tcrb* and *IgH* loci however, it proved difficult to dissociate transcription from chromatin remodeling (61,62). It may be of significance that in CGI-Eμ RC, binding of BRG1 was relatively higher at D_{Q52} segment, that is, the less transcribed but normally one of the most highly recombining D segments (52–54). Our findings show that BRG1 bound the RC despite strongly defective transcription. Moreover, the binding pattern of BRG1 almost mirrored that of RAG1. Thus, at the RC (and the D–J_H domain by large), there are likely instances where chromatin remodeling can substitute for transcription in mediating RSS accessibility. It is conceivable that the RAG complex is recruited to the endogenous *IgH* RC through at least two interwoven though distinct routes, chromatin remodeling and transcription. Each mechanism would determine which of RAG1 or RAG2 binds first. Chromatin remodeling may be more important for RAG1 binding first, whereas transcription (and associated H3K4me3 deposition) will favor recruitment of RAG2. How this model relates to RAG1/RAG2 heterotetramers binding, and whether the model applies to other antigen receptor loci and off-targets (10) remain to be investigated.

Notwithstanding, an intriguing and key finding of the present study was that while the normally Eμ-dependent transcription was severely diminished in CGI-Eμ RC, recruitment of chromatin remodeling complexes was unaffected. This suggests that Eμ controls transcription and chromatin remodeling through distinct mechanisms. This also suggests that chromatin remodeling provided, at least in part, the mechanistic basis for D–J_H recombination in CGI-Eμ RC.

Eμ-dependent DNA methylation of DJ_H intermediates

An interesting finding of this study was that the J_{H1} portion of the rearranged $D_{Q52}J_{H1}$ intermediates was hypermethylated on the CGI-Eμ allele, a pattern that is reminiscent of Eμ-deleted alleles, *i.e.* demethylated D_{Q52} portion and hypermethylated J_{H1} portion (41). Because demethylation of DJ_H intermediates depends on Eμ enhancer (41), we concluded that CGI insertion somehow interfered with the developmentally-regulated, Eμ-dependent demethylation of D_{Q52}–J_{H1} intermediate. In this context, two points need to be highlighted. First, alteration of Eμ demethylating activity on CGI-Eμ alleles occurred despite normal Iμ transcript levels. This may indicate that Eμ demethylating activity is independent of Eμ function as a germline sense promoter. Second, D_{Q52} promoter region remained unmethylated despite an almost transcriptionally silent D_{Q52} promoter, at least as measured by μ0 transcript levels. This is in agreement with the notion that D_{Q52} promoter region has an autonomous, Eμ-independent, demethylating activity (13) that is maintained even in the absence of substantial transcriptional activity. This activity is likely highly confined to the promoter region as it does not target the closeby RSS. Although we cannot exclude the possibility of very limited spreading of methylation from the J_{H1} portion to the RSS on CGI-Eμ alleles, the mechanisms underlying methylation of the RSS and $D_{Q52}J_{H1}$ intermediates are presently unclear, and may be due to defective transcriptional elongation across them, to an effect of the CGI sequence *per se*, or to both. In this regard, it is possible that the demethylating activity of Eμ *per se* is actually intact, just that it takes place as a spreading process which is diluted or sequestered by the high CpG density in the CGI sequence so that it does not reach the rearranged D_{Q52}-J_{H1} segment.

The phylogenetically remote CGI sequence as a transcriptional insulator

Insertion of different insulators upstream of Eμ enhancer led to reduced V_H-DJ_H recombination despite accumulated DJ_H intermediates (42), and this correlated better with strong reduction of DJ_H transcription than with impaired V_H germline transcription (42). A similar trend was seen in CGI-Eμ pro-B cells with the difference that DJ_H transcription was here completely off. This suggests that the ectopic CGI acts as a powerful transcriptional insulator of Eμ enhancer, and strengthens our proposal that short-range control of DJ_H transcription is an important mechanism by which Eμ controls the long-range V_H–DJ_H recombination (42). This does obviously not preclude the involvement of local epigenetic modifications in this process (40,41). Moreover, the insulator function of CGI sequence persists after completion of V_H–DJ_H as transcription derived from the PV_H promoters, also controlled by Eμ, was inhibited.

How did such a phylogenetically remote sequence acquire a strong transcriptional insulator activity within the highly specialized *IgH* RC is striking and remains to be investigated. That this phenomenon is due to greater spacing/distance between Eμ enhancer and its targets is unlikely because insertion of transcriptional insulators of comparable size had different phenotypes (42) pointing to specific, intrinsic characteristics of the ectopic sequences,

notably their CpG content (Supplementary Table S2). The hypothesis that the effect of the ectopic CGI could have been due to its DNA methylation was excluded as it was found essentially un-methylated. This is in agreement with recent studies, which showed that artificial DNA islands with high G+C content and CpG density resist DNA methylation when inserted at a defined site of the embryonic stem cells' genome (63,64). It is also plausible that the ectopic CGI has acquired transcriptional activity generated for instance by internal sequences acting as cryptic and/or CpG islands promoters leading to some transcriptional interference. Another possibility is that the ectopic CGI sequence, though it did not experience selection for binding sites for mammalian transcription factors (63), may fortuitously contain motifs that bind for instance the transcriptional/architectural factor CTCF. Preliminary ChIP experiments argued against this possibility (Supplementary Figure S4). This however does not exclude the possibility that the insertion may have caused the generation of alternative, CTCF-independent, loops that drove Eμ enhancer away from its usual partners (13). Whether these loops involve other transcriptional/architectural factors or other mechanisms that influence the architectural dynamics of the locus are questions for future investigations.

Regardless of the absolute mechanism through which the CGI sequence alters the events taking place at the endogenous *IgH* locus, our study strongly suggests that the insertion affected the transcriptional and the demethylating functions of Eμ enhancer but not its remodeling and recombinational functions. Intact chromatin remodeling likely made RC RSSs accessible to RAG1 first, thus compensating for the defective transcription-associated RAG2 recruitment, and enabling assembly of the RAG complex to initiate D–J_H recombination.

SUPPLEMENTARY DATA

Supplementary Data are available at NAR Online.

ACKNOWLEDGEMENTS

We thank N. Puget for initiating the project, JM Santos for critical reading of the manuscript, Grace Teng (David G. Schatz's lab) for help with RAG ChIP protocol, and the IPBS animal facility and the Imaging Core Facility TRI-IPBS, in particular Emmanuelle Näser, for their excellent work.

FUNDING

Agence Nationale de la Recherche [ANR-16-CE12-0017]; Institut National du Cancer [INCA_9363, PLBIO15-134]; Fondation ARC pour la Recherche sur le Cancer [PJA 20191209515]; Ligue contre le Cancer [Comité de l'ex-Région Midi Pyrénées]; C.O. is a fellow of the Ministry of Higher Education & Research and is recipient of a fellowship from the 'Fondation pour la Recherche Médicale'; Tri-IPBS has the financial support of ITMO Cancer Aviesan (National Alliance for Life Science and Health) within the framework of Cancer Plan. Funding for open access charge: Agence Nationale de la Recherche.

Conflict of interest statement. None declared.

REFERENCES

1. Matthews,A.G. and Oettinger,M.A. (2009) RAG: a recombinase diversified. *Nat. Immunol.*, **10**, 817–821.
2. Schatz,D.G. and Ji,Y. (2011) Recombination centres and the orchestration of V(D)J recombination. *Nat. Rev. Immunol.*, **11**, 251–263.
3. Boboila,C., Alt,F.W. and Schwer,B. (2012) Classical and alternative end-joining pathways for repair of lymphocyte-specific and general DNA double-strand breaks. *Adv. Immunol.*, **116**, 1–49.
4. Roth,D.B. (2014) V(D)J recombination: mechanism, errors, and fidelity. *Microb. Spectr.*, **2**, doi:10.1128/microbiolspec.MDNA3-0041-2014.
5. Chang,H.H.Y., Pannunzio,N.R., Adachi,N. and Lieber,M.R. (2017) Non-homologous DNA end joining and alternative pathways to double-strand break repair. *Nat. Rev. Mol. Cell Biol.*, **18**, 495–506.
6. Liu,Y., Subrahmanyam,R., Chakraborty,T., Sen,R. and Desiderio,S. (2007) A plant homeodomain in RAG-2 that binds Hypermethylated lysine 4 of histone H3 is necessary for efficient antigen-receptor-gene rearrangement. *Immunity*, **27**, 561–571.
7. Matthews,A.G., Kuo,A.J., Ramon-Maiques,S., Han,S., Champagne,K.S., Ivanov,D., Gallardo,M., Carney,D., Cheung,P., Ciccone,D.N. *et al.* (2007) RAG2 PHD finger couples histone H3 lysine 4 trimethylation with V(D)J recombination. *Nature*, **450**, 1106–1110.
8. Shimazaki,N., Tsai,A.G. and Lieber,M.R. (2009) H3K4me3 stimulates the V(D)J RAG complex for both nicking and hairpinning in trans in addition to tethering in cis: implications for translocations. *Mol. Cell*, **34**, 535–544.
9. Ji,Y., Resch,W., Corbett,E., Yamane,A., Casellas,R. and Schatz,D.G. (2010) The in vivo pattern of binding of RAG1 and RAG2 to antigen receptor loci. *Cell*, **141**, 419–431.
10. Teng,G. and Schatz,D.G. (2015) Regulation and evolution of the RAG recombinase. *Adv. Immunol.*, **128**, 1–39.
11. Lin,S.G., Ba,Z., Alt,F.W. and Zhang,Y. (2018) RAG chromatin scanning during V(D)J recombination and chromatin loop extrusion are related processes. *Adv. Immunol.*, **139**, 93–135.
12. Carico,Z. and Krangel,M.S. (2015) Chromatin dynamics and the development of the TCRalpha and TCRdelta repertoires. *Adv. Immunol.*, **128**, 307–361.
13. Kumari,G. and Sen,R. (2015) Chromatin interactions in the control of immunoglobulin heavy chain gene assembly. *Adv. Immunol.*, **128**, 41–92.
14. Proudhon,C., Hao,B., Raviram,R., Chaumeil,J. and Skok,J.A. (2015) Long-range regulation of V(D)J recombination. *Adv. Immunol.*, **128**, 123–182.
15. Majumder,K., Bassing,C.H. and Oltz,E.M. (2015) Regulation of Tcrb gene assembly by genetic, epigenetic, and topological mechanisms. *Adv. Immunol.*, **128**, 273–306.
16. Yancopoulos,G.D. and Alt,F.W. (1985) Developmentally controlled and tissue-specific expression of unrearranged VH gene segments. *Cell*, **40**, 271–281.
17. Bolland,D.J., Wood,A.L., Johnston,C.M., Bunting,S.F., Morgan,G., Chakalova,L., Fraser,P.J. and Corcoran,A.E. (2004) Antisense intergenic transcription in V(D)J recombination. *Nat. Immunol.*, **5**, 630–637.
18. Abarrategui,I. and Krangel,M.S. (2007) Noncoding transcription controls downstream promoters to regulate T-cell receptor alpha recombination. *EMBO J.*, **26**, 4380–4390.
19. Bolland,D.J., Wood,A.L., Afshar,R., Featherstone,K., Oltz,E.M. and Corcoran,A.E. (2007) Antisense intergenic transcription precedes Igh D-to-J recombination and is controlled by the intronic enhancer Emu. *Mol. Cell Biol.*, **27**, 5523–5533.
20. Giallourakis,C.C., Franklin,A., Guo,C., Cheng,H.L., Yoon,H.S., Gallagher,M., Perlot,T., Andzelm,M., Murphy,A.J., Macdonald,L.E. *et al.* (2010) Elements between the IgH variable (V) and diversity (D) clusters influence antisense transcription and lineage-specific V(D)J recombination. *Proc. Natl. Acad. Sci. U.S.A.*, **107**, 22207–22212.
21. Hsieh,C.L., McCloskey,R.P. and Lieber,M.R. (1992) V(D)J recombination on minichromosomes is not affected by transcription. *J. Biol. Chem.*, **267**, 15613–15619.

22. Chen,J., Young,F., Bottaro,A., Stewart,V., Smith,R.K. and Alt,F.W. (1993) Mutations of the intronic IgH enhancer and its flanking sequences differentially affect accessibility of the JH locus. *EMBO J.*, **12**, 4635–4645.
23. Angelin-Duclos,C. and Calame,K. (1998) Evidence that immunoglobulin VH-DJ recombination does not require germ line transcription of the recombining variable gene segment. *Mol. Cell Biol.*, **18**, 6253–6264.
24. Cherry,S.R. and Baltimore,D. (1999) Chromatin remodeling directly activates V(D)J recombination. *Proc. Natl. Acad. Sci. U.S.A.*, **96**, 10788–10793.
25. Goebel,P., Janney,N., Valenzuela,J.R., Romanow,W.J., Murre,C. and Feeney,A.J. (2001) Localized gene-specific induction of accessibility to V(D)J recombination induced by E2A and early B cell factor in nonlymphoid cells. *J. Exp. Med.*, **194**, 645–656.
26. Delpy,L., Decourt,C., Le Bert,M. and Cogne,M. (2002) B cell development arrest upon insertion of a neo gene between JH and Emu: promoter competition results in transcriptional silencing of germline JH and complete VDJ rearrangements. *J. Immunol.*, **169**, 6875–6882.
27. Sikes,M.L., Meade,A., Tripathi,R., Krangel,M.S. and Oltz,E.M. (2002) Regulation of V(D)J recombination: a dominant role for promoter positioning in gene segment accessibility. *Proc. Natl. Acad. Sci. U.S.A.*, **99**, 12309–12314.
28. Jackson,A., Kondilis,H.D., Khor,B., Sleckman,B.P. and Krangel,M.S. (2005) Regulation of T cell receptor beta allelic exclusion at a level beyond accessibility. *Nat. Immunol.*, **6**, 189–197.
29. Du,H., Ishii,H., Pazin,M.J. and Sen,R. (2008) Activation of 12/23-RSS-dependent RAG cleavage by hSWI/SNF complex in the absence of transcription. *Mol. Cell*, **31**, 641–649.
30. Okada,A., Mendelsohn,M. and Alt,F. (1994) Differential activation of transcription versus recombination of transgenic T cell receptor beta variable region gene segments in B and T lineage cells. *J. Exp. Med.*, **180**, 261–272.
31. Fernex,C., Capone,M. and Ferrier,P. (1995) The V(D)J recombinational and transcriptional activities of the immunoglobulin heavy-chain intronic enhancer can be mediated through distinct protein-binding sites in a transgenic substrate. *Mol. Cell Biol.*, **15**, 3217–3226.
32. Hesslein,D.G., Pflugh,D.L., Chowdhury,D., Bothwell,A.L., Sen,R. and Schatz,D.G. (2003) Pax5 is required for recombination of transcribed, acetylated, 5′ IgH V gene segments. *Genes Dev.*, **17**, 37–42.
33. Johnston,C.M., Wood,A.L., Bolland,D.J. and Corcoran,A.E. (2006) Complete sequence assembly and characterization of the C57BL/6 mouse Ig heavy chain V region. *J. Immunol.*, **176**, 4221–4234.
34. Retter,I., Chevillard,C., Scharfe,M., Conrad,A., Hafner,M., Im,T.H., Ludewig,M., Nordsiek,G., Severitt,S., Thies,S. *et al.* (2007) Sequence and characterization of the Ig heavy chain constant and partial variable region of the mouse strain 129S1. *J. Immunol.*, **179**, 2419–2427.
35. Jung,D., Giallourakis,C., Mostoslavsky,R. and Alt,F.W. (2006) Mechanism and control of V(D)J recombination at the immunoglobulin heavy chain locus. *Annu. Rev. Immunol.*, **24**, 541–570.
36. Khamlichi,A.A. and Feil,R. (2018) Parallels between mammalian mechanisms of monoallelic gene expression. *Trends Genet.*, **34**, 954–971.
37. Perlot,T., Alt,F.W., Bassing,C.H., Suh,H. and Pinaud,E. (2005) Elucidation of IgH intronic enhancer functions via germ-line deletion. *Proc. Natl. Acad. Sci. U.S.A.*, **102**, 14362–14367.
38. Afshar,R., Pierce,S., Bolland,D.J., Corcoran,A. and Oltz,E.M. (2006) Regulation of IgH gene assembly: role of the intronic enhancer and 5′DQ52 region in targeting DHJH recombination. *J. Immunol.*, **176**, 2439–2447.
39. Chakraborty,T., Perlot,T., Subrahmanyam,R., Jani,A., Goff,P.H., Zhang,Y., Ivanova,I., Alt,F.W. and Sen,R. (2009) A 220-nucleotide deletion of the intronic enhancer reveals an epigenetic hierarchy in immunoglobulin heavy chain locus activation. *J. Exp. Med.*, **206**, 1019–1027.
40. Subrahmanyam,R., Du,H., Ivanova,I., Chakraborty,T., Ji,Y., Zhang,Y., Alt,F.W., Schatz,D.G. and Sen,R. (2012) Localized epigenetic changes induced by DH recombination restricts recombinase to DJH junctions. *Nat. Immunol.*, **13**, 1205–1212.
41. Selimyan,R., Gerstein,R.M., Ivanova,I., Precht,P., Subrahmanyam,R., Perlot,T., Alt,F.W. and Sen,R. (2013) Localized DNA demethylation at recombination intermediates during immunoglobulin heavy chain gene assembly. *PLoS Biol.*, **11**, e1001475.
42. Puget,N., Hirasawa,R., Hu,N.S., Laviolette-Malirat,N., Feil,R. and Khamlichi,A.A. (2015) Insertion of an imprinted insulator into the IgH locus reveals developmentally regulated, transcription-dependent control of V(D)J recombination. *Mol. Cell Biol.*, **35**, 529–543.
43. Oudinet,C., Braikia,F.Z., Dauba,A., Santos,J.M. and Khamlichi,A.A. (2019) Developmental regulation of DNA cytosine methylation at the immunoglobulin heavy chain constant locus. *PLoS Genet.*, **15**, e1007930.
44. Braikia,F.Z., Conte,C., Moutahir,M., Denizot,Y., Cogne,M. and Khamlichi,A.A. (2015) Developmental switch in the transcriptional activity of a long-range regulatory element. *Mol. Cell Biol.*, **35**, 3370–3380.
45. Santos,J.M., Braikia,F.Z., Oudinet,C., Dauba,A. and Khamlichi,A.A. (2019) Two modes of cis-activation of switch transcription by the IgH superenhancer. *Proc. Natl. Acad. Sci. U.S.A.*, **116**, 14708–14713.
46. Doerfler,W., Weber,S. and Naumann,A. (2018) Inheritable epigenetic response towards foreign DNA entry by mammalian host cells: a guardian of genomic stability. *Epigenetics*, **13**, 1141–1153.
47. Li,B., Carey,M. and Workman,J.L. (2007) The role of chromatin during transcription. *Cell*, **128**, 707–719.
48. Morshead,K.B., Ciccone,D.N., Taverna,S.D., Allis,C.D. and Oettinger,M.A. (2003) Antigen receptor loci poised for V(D)J rearrangement are broadly associated with BRG1 and flanked by peaks of histone H3 dimethylated at lysine 4. *Proc. Natl. Acad. Sci. U.S.A.*, **100**, 11577–11582.
49. Reth,M.G. and Alt,F.W. (1984) Novel immunoglobulin heavy chains are produced from DJH gene segment rearrangements in lymphoid cells. *Nature*, **312**, 418–423.
50. Alessandrini,A. and Desiderio,S.V. (1991) Coordination of immunoglobulin DJH transcription and D-to-JH rearrangement by promoter-enhancer approximation. *Mol. Cell Biol.*, **11**, 2096–2107.
51. Bossen,C., Mansson,R. and Murre,C. (2012) Chromatin topology and the regulation of antigen receptor assembly. *Annu. Rev. Immunol.*, **30**, 337–356.
52. Choi,N.M., Loguercio,S., Verma-Gaur,J., Degner,S.C., Torkamani,A., Su,A.I., Oltz,E.M., Artyomov,M. and Feeney,A.J. (2013) Deep sequencing of the murine IgH repertoire reveals complex regulation of nonrandom V gene rearrangement frequencies. *J. Immunol.*, **191**, 2393–2402.
53. Bolland,D.J., Koohy,H., Wood,A.L., Matheson,L.S., Krueger,F., Stubbington,M.J., Baizan-Edge,A., Chovanec,P., Stubbs,B.A., Tabbada,K. *et al.* (2016) Two mutually exclusive local chromatin states drive efficient V(D)J recombination. *Cell Rep.*, **15**, 2475–2487.
54. Lin,S.G., Ba,Z., Du,Z., Zhang,Y., Hu,J. and Alt,F.W. (2016) Highly sensitive and unbiased approach for elucidating antibody repertoires. *Proc. Natl. Acad. Sci. U.S.A.*, **113**, 7846–7851.
55. Ernst,P. and Smale,S.T. (1995) Combinatorial regulation of transcription II: the immunoglobulin mu heavy chain gene. *Immunity*, **2**, 427–438.
56. Liu,H., Schmidt-Supprian,M., Shi,Y., Hobeika,E., Barteneva,N., Jumaa,H., Pelanda,R., Reth,M., Skok,J. and Rajewsky,K. (2007) Yin Yang 1 is a critical regulator of B-cell development. *Genes Dev.*, **21**, 1179–1189.
57. Bain,G., Maandag,E.C., Izon,D.J., Amsen,D., Kruisbeek,A.M., Weintraub,B.C., Krop,I., Schlissel,M.S., Feeney,A.J., van Roon,M. *et al.* (1994) E2A proteins are required for proper B cell development and initiation of immunoglobulin gene rearrangements. *Cell*, **79**, 885–892.
58. Zhuang,Y., Soriano,P. and Weintraub,H. (1994) The helix-loop-helix gene E2A is required for B cell formation. *Cell*, **79**, 875–884.
59. Dang,W., Sun,X.H. and Sen,R. (1998) ETS-mediated cooperation between basic helix-loop-helix motifs of the immunoglobulin mu heavy-chain gene enhancer. *Mol. Cell Biol.*, **18**, 1477–1488.
60. Spicuglia,S., Kumar,S., Yeh,J.H., Vachez,E., Chasson,L., Gorbatch,S., Cautres,J. and Ferrier,P. (2002) Promoter activation by enhancer-dependent and -independent loading of activator and coactivator complexes. *Mol. Cell*, **10**, 1479–1487.

61. Osipovich,O., Cobb,R.M., Oestreich,K.J., Pierce,S., Ferrier,P. and Oltz,E.M. (2007) Essential function for SWI-SNF chromatin-remodeling complexes in the promoter-directed assembly of Tcrb genes. *Nat. Immunol.*, **8**, 809–816.
62. Osipovich,O.A., Subrahmanyam,R., Pierce,S., Sen,R. and Oltz,E.M. (2009) Cutting edge: SWI/SNF mediates antisense Igh transcription and locus-wide accessibility in B cell precursors. *J. Immunol.*, **183**, 1509–1513.
63. Krebs,A.R., Dessus-Babus,S., Burger,L. and Schubeler,D. (2014) High-throughput engineering of a mammalian genome reveals building principles of methylation states at CG rich regions. *Elife*, **3**, e04094.
64. Wachter,E., Quante,T., Merusi,C., Arczewska,A., Stewart,F., Webb,S. and Bird,A. (2014) Synthetic CpG islands reveal DNA sequence determinants of chromatin structure. *Elife*, **3**, e03397.